Behaviour of Olivine Refractories at High Temperature: Agglomeration in a Fluidized Bed Reactor

EIRICH AWARD 2013

Rudy Michel, Mohamed Ramzi Ammar, Patrick Simon, Emmanuel de Bilbao, Jacques Poirier

Natural olivine is an important refractory raw material because of its abundance in the earth's crust. It is composed of solid solution of magnesium silicate with forsterite Mg_2SiO_4 configuration and iron silicate in a small amount of fayalite Fe_2SiO_4. This raw material is mainly used in different refractory applications. For instance, it is used in fluidized bed reactors to produce a high calorific fuel-rich synthesis gas ($CO + H_2$) from biomass. However, in gasification/combustion reactor, the agglomeration of the fluidized bed may occur due to the reactions between olivine and biomass ashes. Additionally, olivine undergoes phase transformations (dehydration and oxidation) during calcination at high temperature, which significantly affect the chemical processes. Among these phase transformations, magnetite is produced and contributes to the reactivity of refractories as well as to the particle agglomeration with biomass ashes.

1 Introduction

Olivine is an interesting raw material for refractory application due to its abundance and its chemico-physical properties. Natural olivine $(Mg_{0,92},Fe_{0,08})SiO_4$ is an orthosilicate resulting from the complete solid solution between forsterite (Mg_2SiO_4) and in few content fayalite (Fe_2SiO_4). The structure consists of isolated SiO_4^{4-} tetrahedra, where each of the tetrahedra oxygen atoms is shared by three octahedral cations [1]. Olivine is widely used in different industrial fields such as a catalyst in thermal processes [2], as tundish refractory lining for steelmaking [3], and as material for renewable energies [4]. In the field of energy production, olivine is used as raw material in bubbling fluidized bed (BFB) for biomass gasification technologies. It is also used after calcination at high temperature to enhance the mechanical strength and its catalytic aspect [5]. Basically, the fluidized bed reactor technology allows a good distribution of the produced heat (750–900 °C) and a good mixing of fuel, resulting in a homogeneous temperature field. However, the fluidized bed aggregates due to the interaction between the molten biomass ashes, forming new compounds with low melting points (500–1000 °C). The solid particles form agglomerates ensuing from sticking and sintering at high temperature. Then the flow gas upwards becomes insufficient which is a major technical and economical problem for industrial BFB reactors. Therefore, agglomeration is mainly dependent on the bed material and the process temperature, where the high temperature greatly affects the agglomeration processes [6].

There is extensive literature on the enhancement of olivine in terms of chemico-physical and mechanical aspects, for example, calcination treatment [5], metal doping [7], and use of additives [8]. Nevertheless, although the striking feature of olivine was demonstrated, the microscopic mechanisms are not well understood. The academic and industrial objectives of this research are to develop an original laboratory reactor to emulate the agglomeration at high temperature in BFB, to study olivine materials using powerful and complementary techniques (XRD and *Raman* spectroscopy), to clarify the physicochemical mechanism of the interaction with molten ashes and to give practical recommendations to limit the bed defluidization of the renewable energy reactor.

2 Characterization of olivine refractory

Fig. 1 illustrates the in situ high temperature-XRD data of olivine. The hydrated serpentine phase disappears at about 600 °C. Consequently, both forsterite and enstatite phases are expected to be formed after the heat treatment of olivine in air according to the following chemical equation (eq. 1):

$$2Mg_3Si_2O_5(OH)_4 \rightarrow 2Mg_2SiO_4 + 2MgSiO_3 + 4H_2O \qquad (1)$$

New phases are formed as seen by the $2\theta = 23{,}8°$ and $32{,}7°$ peaks between

Rudy Michel, Mohamed Ramzi Ammar, Patrick Simon, Emmanuel de Bilbao, Jacques Poirier
CNRS, CEMHTI UPR3079, Univ. Orléans
45071 Orléans
France

Corresponding author: *Rudy Michel*
E-mail: rudy.michel@cnrs-orleans.fr

Keywords: olivine refractory, fluidized bed, Raman spectrometry, in situ XRD

Received: 31.05.2013
Accepted: 24.09.2013

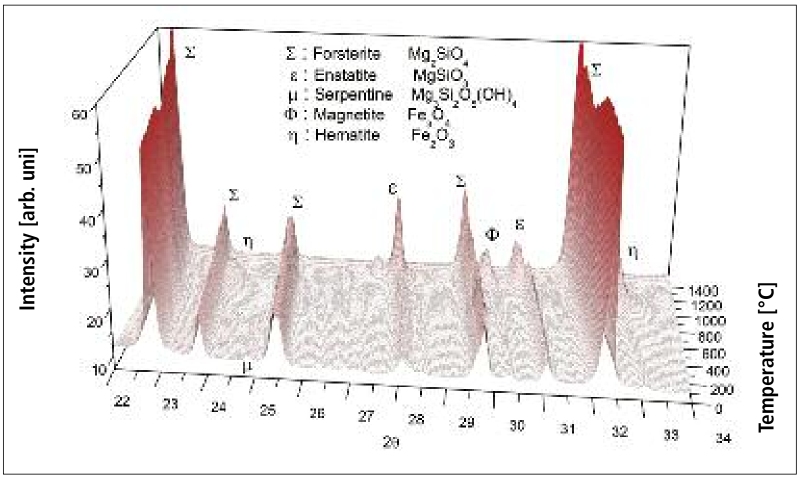

Fig. 1 **In situ HT-XRD of olivine**

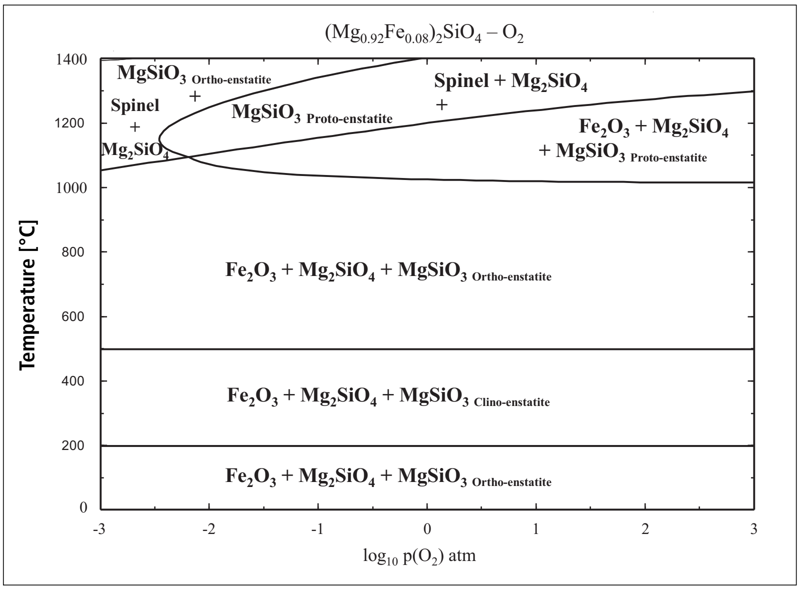

Fig. 2 **Phase diagram of $(Mg_{0,92}Fe_{0,08})2SiO_4 – O_2$, Factsage v6.2**

725 °C and 1150 °C and 2θ = 29,7° between 1150 and 1400 °C. According to the literature, these phases are identified as hematite (2) and magnetite (3):

$$2Fe_2SiO_4 + O_2 \rightarrow 2Fe_2O_3 + 2SiO_2 \qquad (2)$$

$$3Fe_2SiO_4 + O2 \rightarrow 2Fe_3O_4 + 3SiO_2 \qquad (3)$$

Then silica reacts with forsterite to form enstatite according to reaction (4):

$$Mg_2SiO_4 + SiO_2 \rightarrow 2MgSiO_3 \qquad (4)$$

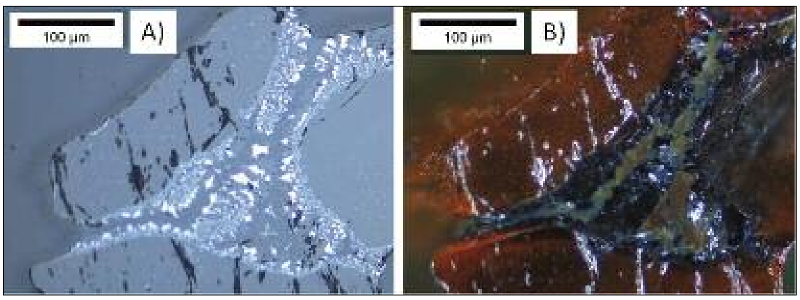

Fig. 3a–b **Micrograph of calcined olivine at 1400 °C/48 h: a) bright field, b) dark field**

The phase transformation of clino-enstatite into proto-enstatite was observed at 1100 °C, mainly at 2θ = 31°. The thermodynamic phase diagram in Fig. 2 determined with Factsage software confirms the experimental data of enstatite observed at high temperature.

3 Reactivity of olivine refractory particles

Fig. 3 displays the micrograph of calcined olivine grains sintered at 1400 °C during 48 h [9]. Three particles are observed and present a red color in the optical micrograph obtained with the dark field mode. The particles are sintered and present a black and brown color which show new phases.

From this micrograph, a Raman mapping was performed and the results are shown in Fig. 4. Raman spectra are sequentially collected, point by point, over a defined region. Then, the maps are reconstructed by a linear combination of spectra from the four pure components contained in the sample. Fig. 4 displays the map of scores of these pure components.

Four phases were detected by Raman mapping. Forsterite is found in the three olivine particles with hematite which gives the red color on the optical micrograph. Magnetite and enstatite are found in the sintered zone. Magnetite is also detected in olivine particle surface.

4 Interactions between ashes and olivine refractory

In this study, the biomass is Miscanthus x giganteus (MXG) and ashes have been investigated. The elemental composition shows the main contributors: Si, K, Ca, Mg, P, S and Cl. These elements are present as KCl, K_2SO_4, K_2HPO_4, $CaCO_3$ and amorphous SiO_2 [10].

The interaction between the ash and the bed were carried out at the laboratory scale in order to observe the morphology and to measure the composition profiles. Ash and olivine samples (natural and calcined at 1400 °/4 h) were first mixed in a platinum crucible and heat-treated during 6 h at 900 °C in a muffle furnace. Subsequently, the samples were embedded in an epoxy resin, polished and finally coated with gold in order to be examined by SEM-EDX (FEG *Hitachi* S4500) [10].

The interaction of ashes and natural olivine are shown in Fig. 5a. The particles of natural olivine (dark areas) surrounded by molten ash can be observed. After interaction with ash at 900 °C during 4 h, 2 % iron is present on the surface of grain into the molten ash. We can suppose a low diffusion of iron from natural olivine to molten ash at high temperature, showing a chemical interaction, which contributes to the agglomeration, while MXG ashes contain only traces of iron (<0,1 mass-%).

Regarding, interaction of miscanthus ashes and calcined olivine in Fig. 5b, strong diffusion of iron is observed. Due to the calcination at 1400 °C, calcined olivine presents iron veins on its surface. Moreover after interaction with ash at 900 °C during 4 h, iron is also present on the surface of grain in contact with the molten ash. This white layer contains 19 mass-% Fe and 17 mass-% K. The composition of molten ash close to the particle surface contains 9 mass-% Fe and 21 mass-% K.

5 Agglomeration in fluidized bed reactor

Recently, the *CEMHTI Laboratory* has developed a new fluidized bed reactor to study the agglomeration effect between Miscanthus ash and olivine. The reactor is made of quartz as shown in Fig. 6a. It is composed of two tubes separated by a quartz grid as shown in Fig. 6b. The reactor is heated by an electrical tubular furnace.

Two kinds of beds were used, natural olivine and calcined olivine at 1400 °C during 4 h. The bed material was sieved between 400–500 µm and fluidized by air at 900 °C for 1,30 h. Fig. 7 presents the agglomeration rate (mass-% particles >500 µm) as a function of the quality of Miscanthus ashes. In the case of calcined olivine, there are more agglomerated particles (× 5) than in the case of natural olivine. This difference is explained by the iron diffusion of calcined olivine showed in the static condition. The iron diffusion promotes agglomeration of olivine.

Some agglomerated particles of natural olivine are shown in the Fig. 8. The picture presents different sizes of agglomerated particles between about 1 mm and 6 mm of diameter.

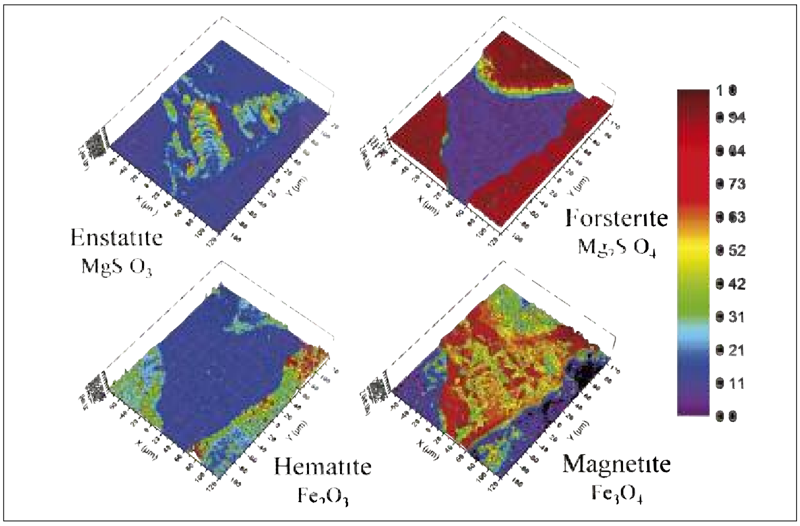

Fig. 4 Raman mapping of calcined olivine sintering

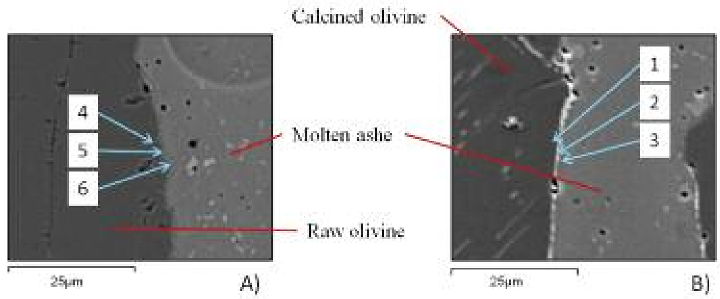

	Mg [mass-%]	Si [mass-%]	K [mass-%]	Fe [mass-%]
1	29,8	26,0	1,3	4,8
2	6,6	24,2	16,9	18,9
3	2,3	29,5	20,5	9,2
4	33	23	/	6
5	5	32	20	2
6	4	34	19	/

Fig. 5a–b SEM-EDX analysis showing the interactions between ash and a) natural olivine and b) calcined olivine

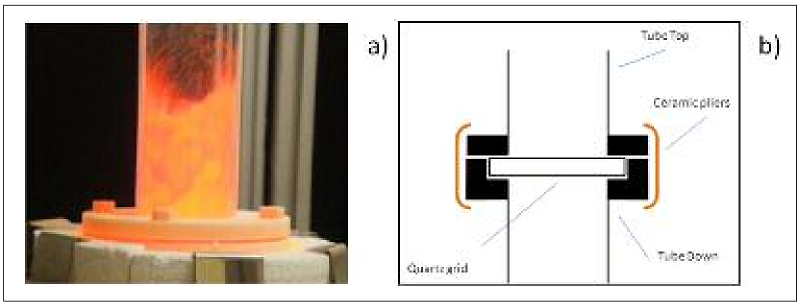

Fig. 6 Reactor made of quartz

6 Conclusion

The understanding of the agglomeration phenomena requires the investigating of inorganic materials and the study of the interaction between bed particles and ash in static then in dynamic conditions.

Regarding the natural olivine, it is composed of $(Mg_{0,92},Fe_{0,08})_2SiO_4$ and transforms at high temperature by dehydration and oxidation of iron.

The static interaction between calcined olivine/ash shows that there is a thin layer of iron containing ash around the bed particles. Thereby, this point shows that iron participates in layer formation via diffusion from the inner part of the olivine grain to the surface.

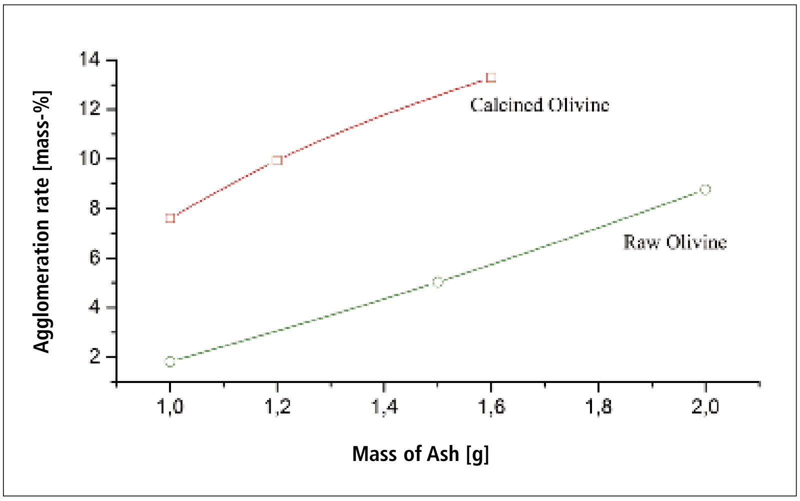

Fig. 7 Agglomeration test in fluidized bed reactor

Fig. 8 Natural olivine agglomerated by MXG ash at 900 °C/2 h

In the case of dynamic interaction, the first test shows sticking of olivine on ash. The agglomeration is more significant in the case of calcined olivine. This effect is due to a higher iron diffusion for calcined olivine.

References

[1] Michel, R.; et al.: Phase transformation characterization of olivine subjected to high temperature in air. Ceram. Int. **39** (2012) 5287–5294

[2] Guillén, M.D.; Dıaz, C.; Blanco, C.G.: Characterization of coal tar pitches with different softening points by 1H NMR Role of the different kinds of protons in the thermal process. Fuel Process. Technol. **58** (1998) 1–15

[3] Lehmann, J.; Boher, M.; Kaerlé, M.C.: An experimental study of the interactions between liquid steel and a MgO-based tundish refractory, Metall. Soc. CIM. **90** (1997) 69–74

[4] Pecho, J.; et al.: Reactive bed materials for improved biomass gasification in a circulating fluidised bed reactor. Chem. Eng. Sci. **63** (2008) 2465–2476

[5] Devi, L.; et al.: Olivine as tar removal catalyst for biomass gasifiers: Catalyst characterization, Appl. Catal. A Gen. **294** (2005) 68–79

[6] Olofsson, G.; et al.: Bed agglomeration problems in fluidized-bed biomass combustion. Ind. Engin. Chem. Res. **41** (2002) 2888–2894

[7] Michel, R.; et al.: Catalytic steam gasification of Miscanthus x giganteus in fluidised bed reactor on olivine based catalysts. Fuel Process. Technol. **92** (2011) 1169–1177

[8] Öhman, M.; Nordin, A.: The role of kaolin in prevention of bed agglomeration during fluidized bed combustion of biomass fuels 2000. Vol. 14, Energy & Fuels 14 (2000) 737–737

[9] Michel, R.; et al.: Phase transformation impact on the iron diffusion in olivine raw material refractory. In: UNITECR Conference, Victoria, Canada, 2013, 1046–1050

[10] Michel, R.; et al.: Physicochemical changes in Miscanthus ash on agglomeration with fluidized bed material. Chem. Engin. J. **207–208** (2012) 497–503